

Dipper discs not inclined towards edge-on orbits

M. Ansdell,^{1★} E. Gaidos,^{2,3} J. P. Williams,¹ G. Kennedy,⁴ M. C. Wyatt,⁴
D. M. LaCourse,[†] T. L. Jacobs[†] and A. W. Mann^{5‡}

¹*Institute for Astronomy, University of Hawai‘i at Mānoa, Honolulu, HI 96822, USA*

²*Department of Geology and Geophysics, University of Hawai‘i at Mānoa, Honolulu, HI 96822, USA*

³*Center for Space and Habitability, University of Bern, CH-3201 Bern, Switzerland*

⁴*Institute of Astronomy, University of Cambridge, Madingley Road, Cambridge CB3 0HA, UK*

⁵*Department of Astronomy, The University of Texas at Austin, Austin, TX 78712, USA*

Accepted 2016 July 13. Received 2016 July 11; in original form 2016 June 12

ABSTRACT

The so-called dipper stars host circumstellar discs and have optical and infrared light curves that exhibit quasi-periodic or aperiodic dimming events consistent with extinction by transiting dusty structures orbiting in the inner disc. Most of the proposed mechanisms explaining the dips – i.e. occulting disc warps, vortices, and forming planetesimals – assume nearly edge-on viewing geometries. However, our analysis of the three known dippers with publicly available resolved sub-mm data reveals discs with a range of inclinations, most notably the face-on transition disc J1604-2130 (EPIC 204638512). This suggests that nearly edge-on viewing geometries are *not* a defining characteristic of the dippers and that additional models should be explored. If confirmed by further observations of more dippers, this would point to inner disc processes that regularly produce dusty structures far above the outer disc mid-plane in regions relevant to planet formation.

Key words: planet–disc interactions – protoplanetary discs – stars: variables: T Tauri, Herbig Ae/Be.

1 INTRODUCTION

Understanding how planets form is one of the most compelling problems in astronomy. Close-in planets appear to be common (Howard et al. 2010; Petigura, Marcy & Howard 2013; Silburt, Gaidos & Wu 2015) and we can study their nascent systems (i.e. protoplanetary discs) in young stellar associations. However, observing planet formation at $\lesssim 1$ au is complicated by small angular scales and faint disc emission compared to the host star; for the nearest star-forming regions, the best achievable angular resolution for optical/infrared scattered light and sub-mm images is only a few au.

However, new probes of the inner disc may be the so-called dipper stars, whose optical and infrared light curves exhibit episodic drops in flux consistent with extinction by transiting dusty structures orbiting with Keplerian periods of down to a few days. Dipper stars were identified with the CoRoT and *Spitzer* missions in the young (~ 2 – 3 Myr) Orion Nebula Cluster (Morales-Calderón et al. 2011) and NGC 2264 region (Alencar et al. 2010; Cody et al. 2014). These studies found that the depth, duration, and periodicity of the dips are consistent with extinction by dust orbiting near the star–disc co-rotation radius. McGinnis et al. (2015) proposed that the

dippers in NGC 2264 could be explained by occulting inner disc warps driven by accretion streams on to the host star, as reported for AA Tau (Bouvier et al. 1999). Unfortunately, the significant distances to these clusters (~ 400 – 750 pc) limits follow-up observations.

Ansdell et al. (2016) identified ~ 25 dippers in the young ($\lesssim 10$ Myr), nearby (~ 120 – 145 Myr) Upper Sco and ρ Oph star-forming regions using high-precision optical photometry from the K2 mission (Howell et al. 2014). Follow-up observations showed that the K2 dippers are often weakly accreting late-type stars hosting moderately evolved primordial discs, challenging the disc warp scenario described above. Thus Ansdell et al. (2016) proposed alternative mechanisms to explain the dips, namely occulting vortices at the inner disc edge produced by the Rossby Wave Instability and transiting clumps of circumstellar material related to planetesimal formation. Bodman et al. (2016) also found that magnetospheric truncation of weakly accreting discs with misaligned magnetic fields could form occulting accretion streams that produce dippers with high to moderate inclinations.

The proposed mechanisms for explaining the dips therefore assume geometries that are closer to edge-on than face-on. The occurrence rate of dippers in co-eval clusters (e.g. ~ 20 – 30 per cent of classical T Tauri stars in NGC 2264; Alencar et al. 2010, Cody et al. 2014) and the moderate optical extinction towards these objects ($A_V \lesssim 1$; Ansdell et al. 2016) suggest that we are not seeing the discs directly edge-on ($i = 90^\circ$), but rather viewing the dippers at

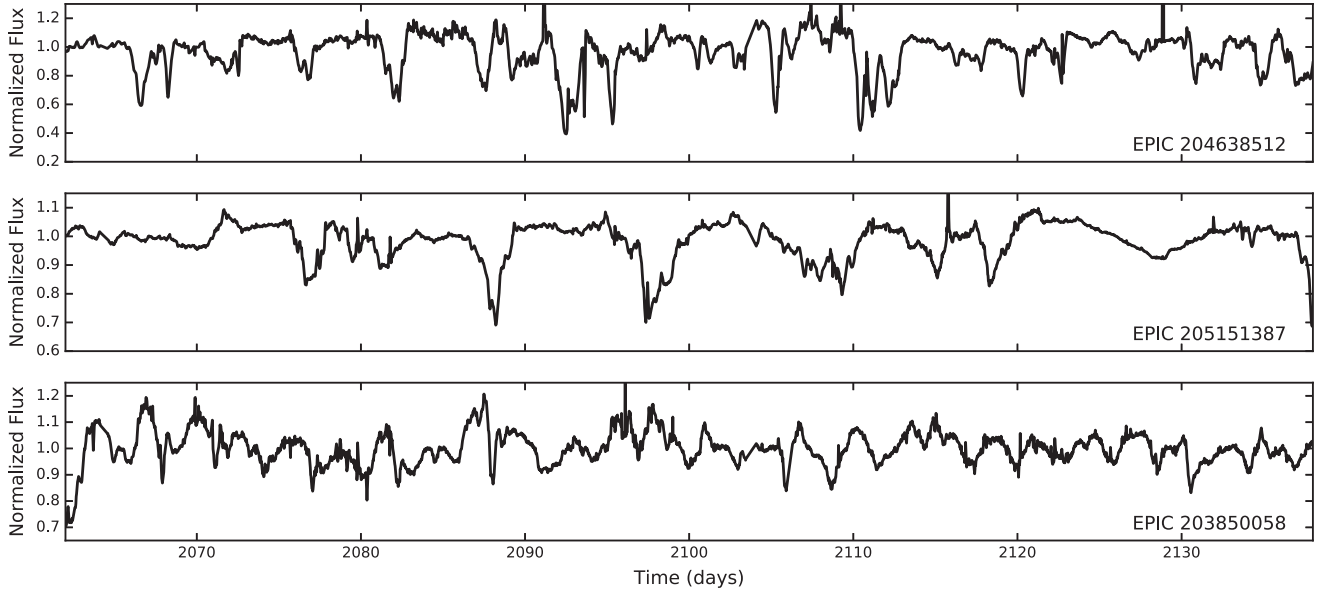
* E-mail: megan.ansdell@gmail.com

† Amateur Astronomer.

‡ Hubble Fellow.

Table 1. Properties of dippers with resolved sub-mm images.

EPIC	2MASS	RA _{J2000}	Dec _{J2000}	Mem.	SpT	T_{eff} (K)	A_V (mag)	Disc	P_{rot} (d)	D_{dip}	Var.
204638512	16042165-2130284	16:04:21.655	-21:30:28.50	USc	K2	4900	0.7	TD	5.00	0.57	A
205151387	16090075-1908526	16:09:00.762	-19:08:52.70	USc	M1	4000	0.8	Full	9.55	0.31	Q
203850058	16253849-2613540	16:27:06.596	-24:41:48.84	Oph	M6	2700	3.0	Full	2.88	0.18	Q

**Figure 1.** Normalized K2 light curves (Section 3.1) showing $\gtrsim 10$ per cent dip depths with ~ 0.5 – 2 d durations typical of dipper stars.

nearly edge-on inclinations (e.g. $i = 70^\circ$) and thus observing transits of dusty structures lifted above the disc mid-plane. However, these geometric assumptions have not yet been compared to observations.

In this Letter, we present the three known dippers whose circumstellar discs have been resolved in archival sub-mm data such that their inclinations can be constrained. Surprisingly, we find discs with a range of inclinations, most notably the face-on transition disc (TD) J1604-2130 (Mathews, Williams & Ménard 2012; Zhang et al. 2014). This indicates that nearly edge-on disc inclinations are *not* a defining characteristic of the dippers, and motivates a re-examination of the dipper mechanisms so that we can properly interpret these objects in the context of planet formation.

2 SAMPLE

Our sample consists of the three dippers with publicly available high-resolution sub-mm data sufficient to constrain disc inclinations. The dippers were identified from their K2 light curves and are located in the ~ 10 -Myr old Upper Sco (Pecaut, Mamajek & Bubar 2012) and ~ 1 -Myr old ρ Oph (Andrews & Williams 2007) star-forming regions. EPIC 205151387 and EPIC 203850058 were reported in Ansdell et al. (2016), while EPIC 204638512 is a newly identified dipper. To our knowledge, these are the only currently known dippers with resolved sub-mm data. Table 1 gives their Ecliptic Plane Input Catalog (EPIC) and Two Micron All-Sky Survey (2MASS; Skrutskie et al. 2006) names, right ascension and declination, cluster membership (Mem.), spectral type (SpT), effective temperature (T_{eff}), optical extinction (A_V), and disc type (Disc). Stellar properties are from the literature (Natta et al. 2002; Carpenter, Ricci & Isella 2014; Ansdell et al. 2016).

EPIC 204638512 is a K-type pre-main-sequence star with spectroscopic signatures of weak accretion (e.g. Dahm, Slesnick & White 2012) and hosts the face-on TD known as J1604-2130 (Mathews et al. 2012; Zhang et al. 2014). EPIC 205151387 is a pre-main-sequence M1 star that hosts a full disc (Carpenter et al. 2014) and exhibits variable accretion signatures (Dahm et al. 2012; Ansdell et al. 2016). EPIC 203850058 is the brown dwarf ρ Oph 102, which hosts a well-studied full disc (Natta et al. 2002; Ricci et al. 2012) that shows evidence for significant mass accretion as well as winds and molecular outflows (Natta et al. 2004; Whelan et al. 2005; Phan-Bao et al. 2008; McClure et al. 2010; Manara et al. 2015).

3 DATA & ANALYSIS

3.1 K2 optical light curves

Fig. 1 presents the K2 light curves of the three dippers in our sample. As in Ansdell et al. (2016), we use the K2SFF light curves made publicly available by the Mikulski Archive for Space Telescopes (MAST). These light curves were extracted from the *Kepler* Target Pixel Files (TPFs) using photometric apertures with the Self Field Flattening (SFF) technique, which corrects for spacecraft motion by correlating observed flux variability with spacecraft pointing (Vanderburg & Johnson 2014).

For EPIC 204638512 and EPIC 205151387, fainter secondary sources are visible within their K2SFF photometric apertures. However, these potentially contaminating interlopers are at sufficiently large projected distances (> 8 arcsec) from the primary targets that their separate light curves can be manually extracted. We obtained the TPFs from MAST and used the *KEP*PCA pipeline to apply

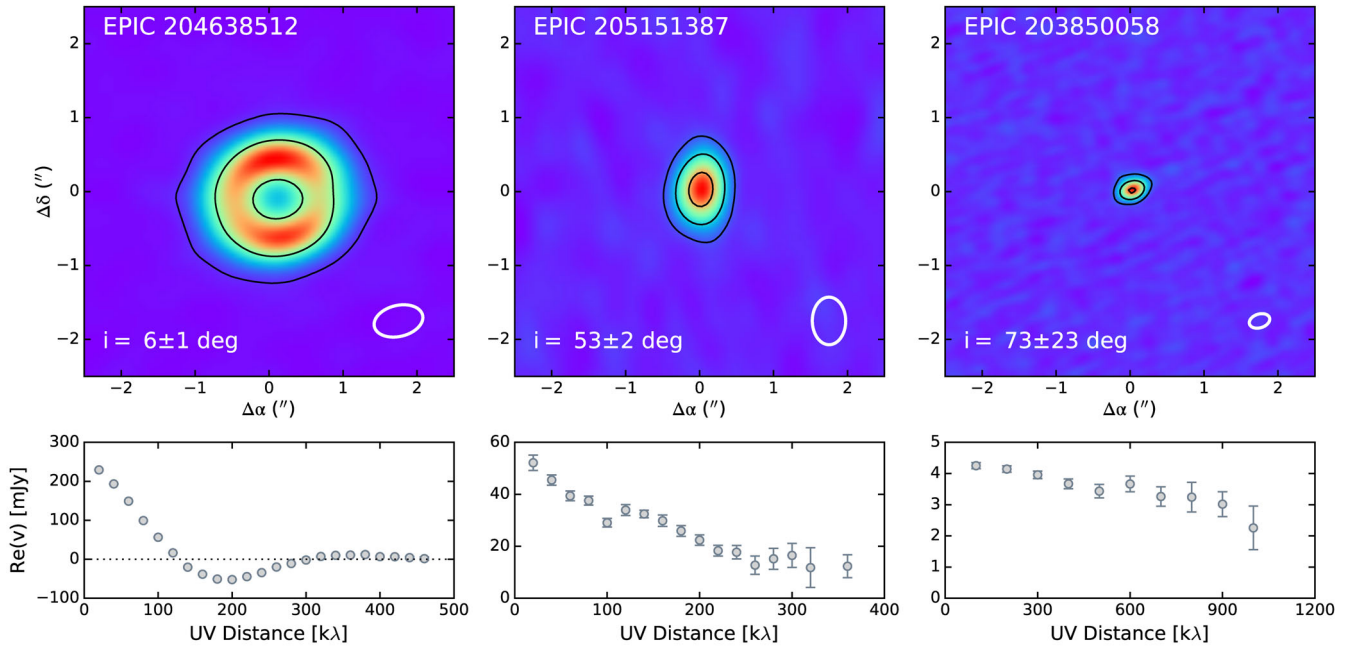


Figure 2. Top panels show ALMA sub-mm continuum images (5 arcsec \times 5 arcsec) with fitted disc inclinations and beam sizes (Sections 3.2 and 4.1). Contours are 10σ and 100σ for EPIC 204638512 and 5σ , 20σ , and 50σ for EPIC 205151387 and EPIC 203850058. Bottom panels show the real part of the visibilities as a function of projected baseline length.

custom photometric apertures for individually extracting the light curves of the primary and secondary sources while also correcting for spacecraft motion. We confirmed that the dipper activity is associated with the primary target with negligible contributions from the secondary source in both cases. We use the K2SFF light curves in the remainder of this work, as they show improved pointing error corrections compared to the light curves produced by our KEPPCA pipeline.

We used the K2 light curves to infer stellar rotation periods (P_{rot}) and characterize the dipper activity in terms of dip depth (D_{dip}) and quasi-periodic (Q) or aperiodic (A) variability (see section 2.2 in Ansdell et al. 2016). Table 1 provides these dipper properties, though the P_{rot} of EPIC 204638512 is uncertain due to a weak rotational signal. The three dippers in our sample generally follow the trends with stellar and disc properties identified in Ansdell et al. (2016), indicating that they are not unusual among the overall dipper population. In particular, they follow the correlation between extinction-corrected *WISE*-2 excess and D_{dip} (see fig. 9 in Ansdell et al. 2016), which was interpreted as evidence that the dips are related to hot inner (rather than cool outer) disc material. The three dippers also follow the observed correlation between P_{rot} and T_{eff} , although EPIC 205151387 has a long P_{rot} for its T_{eff} value. SED modelling by Ansdell et al. (2016) also showed that dippers typically have inner dust discs extending to within a few stellar radii. The infrared colour excesses for EPIC 205151387 and EPIC 203850058 indicate they host full discs (see fig. 6 in Ansdell et al. 2016). Although EPIC 204638512 hosts a disc with a large inner cavity in the sub-mm, it exhibits variable infrared excess consistent with dust at small ($\lesssim 0.1$ au) orbital radii (Dahm 2010; Zhang et al. 2014).

3.2 Resolved sub-mm data

EPIC 204638512 hosts the well-characterized face-on TD known as J1604-2130, which was discovered by Mathews et al. (2012) using

the Sub-millimeter Array (SMA; Ho, Moran & Lo 2004). Mathews et al. (2012) resolved a ~ 70 -au inner dust cavity in their continuum map and derived a precise disc inclination of $6^\circ \pm 1.5^\circ$ using their ^{12}CO 3–2 first-moment map. Zhang et al. (2014) later compared the dust and gas radial structures using ALMA Cycle 0 observations; Fig. 2 shows the cleaned 880 μm continuum image from the ALMA Science Archive (project code: 2011.0.00526.S) with a clearly resolved source and 0.67 arcsec \times 0.42 arcsec (~ 100 au \times 60 au) beam.

EPIC 205151387 was also observed during ALMA Cycle 0 (project code: 2011.0.00526.S) in the 880 μm continuum and ^{12}CO 3–2 line (Carpenter et al. 2014). Fig. 2 shows the cleaned continuum image from the ALMA Science Archive with a 0.64 arcsec \times 0.45 arcsec (~ 95 au \times 65 au) beam. We also plot the real part of the visibilities as a function of projected baseline length, where the clear decrease in visibility with UV distance indicates a spatially resolved source.

EPIC 203850058 was imaged at high resolution in the 870 μm continuum during ALMA Cycle 1 (project code: 2012.1.00046.S). The calibrated continuum data were not available from the ALMA Science Archive, thus we downloaded the raw visibilities and executed the pipeline calibration script, then extracted the continuum image by averaging over the continuum channels and interactively cleaning with a Briggs robust weighting parameter of $+0.5$, giving a beam size of 0.28 arcsec \times 0.19 arcsec (~ 35 au \times 25 au). Fig. 2 shows the cleaned continuum image and the real part of the visibilities as a function of projected baseline length; the slight decrease in the visibilities indicates a marginally resolved source.

3.3 Adaptive optics imaging

We searched the literature for adaptive optics (AO) imagery to check whether close companions could be influencing the dips. EPIC 204638512 has been imaged extensively with AO, providing

strict limits on close companions. Kraus et al. (2008) used aperture masking interferometry combined with direct imaging to rule out the presence of close companions from $\sim 0.07 M_{\odot}$ at ~ 2 au to $\sim 0.02 M_{\odot}$ at ~ 40 au. Ireland et al. (2011) used direct imaging to limit companions from $\sim 0.07 M_{\odot}$ at ~ 60 au to $\sim 0.005 M_{\odot}$ at $\gtrsim 300$ au. High-resolution optical spectroscopy showed no evidence for a double-line spectroscopic binary (Dahm et al. 2012).

EPIC 205151387 also has strict limits on close companions from extensive AO imaging. Companions are ruled out from $\sim 0.03 M_{\odot}$ at ~ 2 au to $\sim 0.01 M_{\odot}$ at ~ 40 au (Kraus et al. 2008) and from $\sim 0.10 M_{\odot}$ at ~ 60 au to $\sim 0.008 M_{\odot}$ at $\gtrsim 300$ au (Ireland et al. 2011). High-resolution optical spectroscopy showed no signs of a double-line spectroscopic binary (Dahm et al. 2012).

EPIC 203850058 is an ultra-cool brown dwarf, making it a particularly difficult target for AO imaging. We do not know of any existing AO data for this source.

4 DISCUSSION

4.1 Disc inclinations

For EPIC 204638512, we adopt the disc inclination of $i = 6^{\circ} \pm 1.5^{\circ}$ derived by Mathews et al. (2012), who placed strong constraints on disc geometry using their ^{12}CO first-moment map and assumptions of Keplerian rotation. For EPIC 205151387 and EPIC 203850058, we derive disc inclinations from their sub-mm continuum data (Section 3.2) using standard routines from the *Common Astronomy Software Applications* (CASA) package (McMullin et al. 2007); although their existing CO data were insufficient to derive precise disc inclinations, the first-moment maps can be used as rough checks on our continuum results.

We derived the disc inclination of EPIC 205151387 using the CASA routine `uvmodelfit`, which fits simple analytic source component models (point-source, Gaussian, or disc) directly to the visibility data. We assumed an elliptical Gaussian model, which has six free parameters: integrated flux density (F), FWHM along the major axis (a), aspect ratio of the axes (r), position angle (PA), right ascension offset from the phase centre ($\Delta\alpha$), and declination offset from the phase centre ($\Delta\delta$). We found $F = 49.5 \pm 0.4$ mJy and PA = $-22^{\circ} \pm 3^{\circ}$, then derived the inclination from r assuming circular disc structure, finding $i = 53^{\circ} \pm 2^{\circ}$. To check our results, we analysed the first-moment ^{12}CO map, finding a similar position angle (PA $\approx -30^{\circ}$) and inclination ($i \approx 50^{\circ}$) when assuming Keplerian rotation.

EPIC 203850058 is thought to have a high disc inclination based on the detection of an optical jet (Whelan et al. 2005) and the nearly symmetric morphology of a bipolar outflow in molecular CO (Phan-Bao et al. 2008), as previously noted by Ricci et al. (2012). To derive an inclination, we again used `uvmodelfit` to fit an elliptical Gaussian model to the continuum visibility data, but with an initial guess of PA $\approx 20^{\circ}$ based on the first-moment ^{12}CO map in Ricci et al. (2012). We found $F = 4.0 \pm 0.1$ mJy and PA = $15^{\circ} \pm 1^{\circ}$, consistent with Ricci et al. (2012). We then derived the inclination from r assuming circular disc structure, finding $i \approx 90^{\circ}$, but with very large errors. We therefore checked our results with the CASA routine `imfit`, which fits an elliptical Gaussian to the source in its image plane, then uses the clean beam to return de-convolved fit results; we found a nearly edge-on disc with $i = 73^{\circ} \pm 23^{\circ}$, $F = 4.2 \pm 0.1$ mJy, and PA = $10^{\circ} \pm 15^{\circ}$. Although the small size and faint emission of this source complicates the analysis, the overall picture appears to point to a nearly edge-on viewing geometry for EPIC 203850058.

Note that these sub-mm observations have resolutions of ~ 20 – 50 au in radius (Section 3.2), thus the estimated inclinations reflect bulk disc geometry and assume a uniform inclination angle throughout the disc. Moreover, the uncertainties do not include systematic errors (e.g. we assume the observed discs of EPIC 205151387 and EPIC 203850058 are adequately represented by elliptical Gaussians).

4.2 A call for re-thinking dipper mechanisms

The proposed mechanisms explaining the dipper phenomenon favour geometries that are nearly edge-on. The discs are likely not seen completely edge-on ($i = 90^{\circ}$), however, due to the moderate extinction towards the dippers ($A_V \lesssim 1$; Ansdell et al. 2016). Rather, it is thought that we are viewing the dippers at nearly edge-on inclinations (e.g. $i = 70^{\circ}$) and thus observing transits of occulting material lifted above the disc mid-plane by some process (e.g. the breakdown of Rossby waves into vortices; Ansdell et al. 2016). Notably, none of the proposed dipper mechanisms can account for obscurations from face-on discs.

Thus the surprising range of dipper disc inclinations presented in this work, in particular the face-on geometry of EPIC 204638512 (J1604-2130), suggests that nearly edge-on viewing geometries are *not* a defining characteristic of the dippers and motivates the exploration of alternative models (or combinations of models) that can explain a range of disc inclinations. For example, occulting accretion streams (e.g. McGinnis et al. 2015; Bodman et al. 2016) could possibly account for even face-on outer discs if they act in concert with other mechanisms warping the inner disc, such as dynamical interactions with (proto-) planets or low-mass stellar companions (e.g. Facchini, Ricci & Lodato 2014; Marino, Perez & Casassus 2015). Populations of scattered planetesimals from migrating (proto-) planets may also explain low dipper disc inclinations (Krijt & Dominik 2011), but more work is needed to explore nearly polar orbits.

4.3 EPIC 204638512 (J1604-2130)

EPIC 204638512 is a particularly interesting case. This source hosts a face-on disc ($i = 6^{\circ} \pm 1.5^{\circ}$; Mathews et al. 2012) with a large sub-mm dust cavity (~ 80 au in radius; Zhang et al. 2014), which seemingly makes it an unlikely dipper. Yet, EPIC 204638512 exhibits the deepest flux dips among the known K2 dippers (up to ~ 60 per cent; Fig. 1). How can these characteristics be reconciled?

The dipper activity may be related to an inclined and variable inner dust disc, as implied from its infrared emission. The object's *Spitzer* IRAC photometry shows no excess (Mathews et al. 2012), while its *Spitzer* IRS spectrum and *WISE* photometry reveal excesses consistent with dust at small ($\lesssim 0.1$ au) orbital radii (Dahm 2010; Zhang et al. 2014). A factor of 4 variability in mid-infrared flux was also seen over several weeks, indicating a rapidly changing inner dust disc (Dahm & Carpenter 2009). Moreover, Takami et al. (2014) used near-infrared imaging polarimetry to identify intensity nulls in the outer disc annulus, which could be self-shadowing from a misaligned inner disc.

An inclined transient inner disc has been proposed for HD 142527, which also hosts a face-on transition disc with a large inner dust gap (Fukagawa et al. 2006) and exhibits intensity nulls along the outer disc annulus in its infrared scattered light images (Casassus et al. 2012). HD 142527 has a known inner disc, thought to be a transient feature of accretion from the outer disc (Verhoeff et al. 2011; Casassus et al. 2013). Marino et al. (2015) modelled the system, finding a relative inclination of $\sim 70^{\circ}$ between the inner and

outer discs, possibly due to dynamical interactions with a low-mass stellar companion orbiting inside the dust gap (Biller et al. 2012; Close et al. 2014; Rodigas et al. 2014).

A similar scenario for EPIC 204638512 would reconcile its dips and face-on outer disc. One indication of an inclined inner disc is EPIC 204638512's weak rotational signal (Section 3.1), which suggests the star is pole-on and thus aligned with the outer disc. The dust cavity of EPIC 204638512 is also thought to have been cleared by giant planet(s) orbiting inside the dust gap (Mathews et al. 2012; Zhang et al. 2014; van der Marel et al. 2015), which could drive an inner disc warp. However, giant planets alone likely cannot account for all the dippers, as dipper occurrence rates (e.g. ~ 20 – 30 per cent in NGC 2264; Alencar et al. 2010, Cody et al. 2014) are much larger than giant planet occurrence rates around late-type stars (e.g. a few per cent; see fig. 8 in Gaidos et al. 2013).

5 SUMMARY

We presented disc inclinations for the three known dippers with resolved sub-mm data. We found discs with a range of viewing geometries, most notably the face-on transition disc J1604-2130. Our findings show that nearly edge-on disc inclinations are *not* a defining characteristic of the dippers, contrary to the currently proposed mechanisms explaining the dips, suggesting that additional models should be explored. Resolving more dipper discs with ALMA, and exploring techniques such as spectroastrometry that can directly probe the inner disc (e.g. Pontoppidan et al. 2008), will be essential to understanding and properly interpreting the dippers in the context of planet formation.

ACKNOWLEDGEMENTS

Support comes from NSF grant AST-1208911 (MA), NASA grants NNX11AC33G (EG) and NNX15AC92G (JPW), ERC grant 279973 (MCW), Hubble Fellowship 51364 (AWM), and a Royal Society University Research Fellowship (GK). This paper makes use of the following ALMA data: ADS/JAO.ALMA#2011.0.00526.S. ALMA is a partnership of ESO (representing its member states), NSF (USA) and NINS (Japan), together with NRC (Canada), NSC and ASIAA (Taiwan), and KASI (Re-public of Korea), in cooperation with the Republic of Chile. The Joint ALMA Observatory is operated by ESO, AUI/NRAO and NAOJ. The National Radio Astronomy Observatory is a facility of the National Science Foundation operated under cooperative agreement by Associated Universities, Inc.

REFERENCES

P.Alencar S. H. et al., 2010, A&A, 519, A88
 Andrews S. M., Williams J. P., 2007, ApJ, 671, 1800
 Ansdell M. et al., 2016, ApJ, 816, 69
 Biller B. et al., 2012, ApJ, 753, L38
 Bodman E. H. L. et al., 2016, preprint (arXiv:1605.03985)

Bouvier J. et al., 1999, A&A, 349, 619
 Carpenter J. M., Ricci L., Isella A., 2014, ApJ, 787, 42
 Casassus S., Perez M. S., Jordán A., Ménard F., Cuadra J., Schreiber M. R., Hales A. S., Ercolano B., 2012, ApJ, 754, L31
 Casassus S. et al., 2013, Nature, 493, 191
 Close L. M. et al., 2014, ApJ, 781, L30
 Cody A. M. et al., 2014, AJ, 147, 82
 Dahm S. E., 2010, AJ, 140, 1444
 Dahm S. E., Carpenter J. M., 2009, AJ, 137, 4024
 Dahm S. E., Slesnick C. L., White R. J., 2012, ApJ, 745, 56
 Facchini S., Ricci L., Lodato G., 2014, MNRAS, 442, 3700
 Fukagawa M., Tamura M., Itoh Y., Kudo T., Imaeda Y., Oasa Y., Hayashi S. S., Hayashi M., 2006, ApJ, 636, L153
 Gaidos E., Fischer D. A., Mann A. W., Howard A. W., 2013, ApJ, 771, 18
 Ho P. T. P., Moran J. M., Lo K. Y., 2004, ApJ, 616, L1
 Howard A. W. et al., 2010, Science, 330, 653
 Howell S. B. et al., 2014, PASP, 126, 398
 Ireland M. J., Kraus A., Martinache F., Law N., Hillenbrand L. A., 2011, ApJ, 726, 113
 Kraus A. L., Ireland M. J., Martinache F., Lloyd J. P., 2008, ApJ, 679, 762
 Krijt S., Dominik C., 2011, A&A, 531, A80
 McClure M. K. et al., 2010, ApJS, 188, 75
 McGinnis P. T. et al., 2015, A&A, 577, A11
 McMullin J. P., Waters B., Schiebel D., Young W., Golap K., 2007, in Shaw R. A., Hill F., Bell D. J., eds, ASP Conf. Ser. Vol. 376, Astronomical Data Analysis Software and Systems XVI. Astron. Soc. Pac., San Francisco, p. 127
 Manara C. F., Testi L., Natta A., Alcalá J. M., 2015, A&A, 579, A66
 Marino S., Perez S., Casassus S., 2015, ApJ, 798, L44
 Mathews G. S., Williams J. P., Ménard F., 2012, ApJ, 753, 59
 Morales-Calderón M. et al., 2011, ApJ, 733, 50
 Natta A., Testi L., Comerón F., Oliva E., D'Antona F., Baffa C., Comoretto G., Gennari S., 2002, A&A, 393, 597
 Natta A., Testi L., Muzerolle J., Randich S., Comerón F., Persi P., 2004, A&A, 424, 603
 Pecaute M. J., Mamajek E. E., Bubar E. J., 2012, ApJ, 746, 154
 Petigura E. A., Marcy G. W., Howard A. W., 2013, ApJ, 770, 69
 Phan-Bao N. et al., 2008, ApJ, 689, L141
 Pontoppidan K. M., Blake G. A., van Dishoeck E. F., Smette A., Ireland M. J., Brown J., 2008, ApJ, 684, 1323
 Ricci L., Testi L., Natta A., Scholz A., de Gregorio-Monsalvo I., 2012, ApJ, 761, L20
 Rodigas T. J., Follette K. B., Weinberger A., Close L., Hines D. C., 2014, ApJ, 791, L37
 Silburt A., Gaidos E., Wu Y., 2015, ApJ, 799, 180
 Skrutskie M. F. et al., 2006, AJ, 131, 1163
 Takami M. et al., 2014, ApJ, 795, 71
 van der Marel N., van Dishoeck E. F., Bruderer S., Pérez L., Isella A., 2015, A&A, 579, A106
 Vanderburg A., Johnson J. A., 2014, PASP, 126, 948
 Verhoeff A. P. et al., 2011, A&A, 528, A91
 Whelan E. T., Ray T. P., Bacciotti F., Natta A., Testi L., Randich S., 2005, Nature, 435, 652
 Zhang K., Isella A., Carpenter J. M., Blake G. A., 2014, ApJ, 791, 42

This paper has been typeset from a $\text{\TeX}/\text{\LaTeX}$ file prepared by the author.